Theoretical Modeling of Compression Effects in Enzymic Methyl Transfer

Ian H. Williams[1]

Contribution from the University Chemical Laboratory, Lensfield Road, Cambridge CB2 1EW, United Kingdom. *Received February 1, 1984*

Abstract: The energetics of catalysis of methyl transfer in a degenerate displacement of methylammonium ion by ammonia via a symmetric S_N2 transition structure have been investigated by ab initio calculations at the 4-31G level of SCF-MO theory for catalyzed and uncatalyzed processes. The model catalyst comprises (a) a pair of helium atoms located a fixed distance apart on the N···C···N axis so as to compress the reacting system by repulsive (destabilizing) interactions and (b) a cage of point charges serving to stabilize both the reactant ion-molecule complex and the transition structure by attractive interactions. Schowen's hypothesis concerning the possible role of compression in enzymic catalysis of methyl transfer is examined. It is shown that the model with compression permits catalysis by preferential transition-state binding of the substrate to the catalyst, but in the absence of compression there is anti-catalysis. Kinetic isotope effects calculated for catalyzed and uncatalyzed model reactions are in accord with trends in experimental isotope effects for enzymic and non-enzymic methyl transfers.

Methyl-group transfer from an electrophile to a nucleophile by an S_N2 mechanism is an archetypical reaction in organic chemistry[2] and still the subject of much experimental[3] and theoretical[4] study. Transmethylation from *S*-adenosylmethionine to a wide range of acceptors is an important process in biochemistry,[5,6] and the mechanism of its enzymic catalysis is of great interest.

The kinetic α-deuterium isotope effect $V^{CH_3}/V^{CD_3} = 0.83 \pm 0.05$ for methylation of 3,4-dihydroxyacetophenone with *S*-adenosylmethionine at 37 °C catalyzed by the enzyme catechol *O*-methyl transferase[7] is more inverse than the isotope effect $(k(CH_3)/k(CD_3) = 0.97 \pm 0.02$ for methylation of methoxide ion by *S*-methyldibenzothiophenium ion at 25 °C in methanol.[8] Schowen and co-workers have interpreted[7] this observation in terms of a tighter S_N2 transition state for the enzyme-catalyzed reaction than for the non-enzymic reaction and have performed[9] model vibrational analysis calculations with empirical force fields to generate semiquantitative information regarding the relative structures of these transition states. The results of this study[9] are consistent with equal Pauling bond orders[10] for the making O···C and breaking C···S bonds of ~0.55 and ~0.45 in the enzymic and non-enzymic transition states, respectively, corresponding to a shortening of ~0.06 Å for each of these bonds in the enzymic relative to the non-enzymic transition state. Schowen has suggested[5] that, as a consequence of this (intrinsically unfavorable) compression of the S_N2 transition state in the enzymic reaction, the enzyme is able to distinguish the transition state structurally from the preceding reactant state and the succeeding product state in order to stabilize the transition state specifically. Thus compression by a methyl transfer enzyme may serve to achieve efficient catalysis, with a large V_{max} at the expense of a slight reduction in V_{max}/K_m, provided that compression of the transition state is energetically less unfavorable than compression of the reactant state in the enzyme-substrate complex.

Scheme I

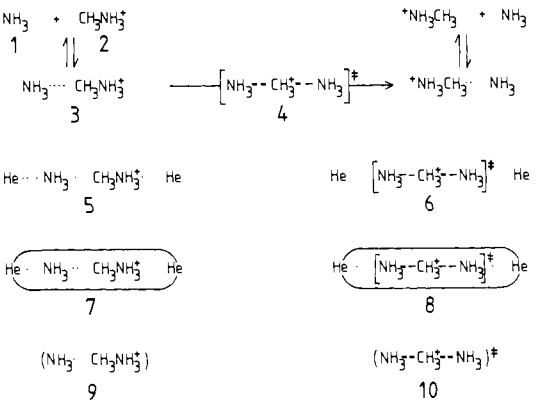

This paper reports a theoretical modeling study designed to investigate Schowen's hypothesis for enzymic methyl transfer. The structural and energetic consequences of compression are examined in relation to a simple methyl transfer process, using non-empirical methods, and the nature of the catalysis is discussed.

Modeling Methods

Ab initio SCF-MO calculations were performed by using the Cambridge Mark 1 version of the HONDO program[11] as implemented on the IBM 3081 computer at the Cambridge University Computing Service. The basis sets employed were 4-31G for carbon, nitrogen, and hydrogen atoms[12] and STO-2G for helium atoms.[13] Geometry optimizations were performed by using either the Murtagh-Sargent[14] or the Schlegel[15] algorithms employing analytical gradients, and Cartesian force constants were determined by numerical differentiation of the gradient by using either a central-difference[16] or a Simplex[17] method. Translational and

(1) Royal Society Pickering Research Fellow.
(2) Albery, W. J.; Kreevoy, M. M. *Adv. Phys. Org. Chem.* **1978**, *16*, 87-147.
(3) Wong, O. S.-L.; Schowen, R. L. *J. Am. Chem. Soc.* **1983**, *105*, 1931-1934.
(4) Chandrasekhar, J.; Smith, S. F.; Jorgensen, W. L. *J. Am. Chem. Soc.* **1984**, *106*, 3049-3050.
(5) Olsen, J.; Wu, Y.-S.; Borchardt, R. T.; Schowen, R. L. In "Transmethylation"; Usdin, E., Borchardt, R. T., Creveling, C. R., Eds.; Elsevier: New York, 1979.
(6) Borchardt, R. T.; Creveling, C. R.; Usdin, E., Eds. "Biochemistry of *S*-Adenosylmethionine and Related Compounds"; MacMillan: New York, 1982.
(7) Hegazi, M. F.; Borchardt, R. T.; Schowen, R. L. *J. Am. Chem. Soc.* **1979**, *101*, 4359-4365.
(8) Gray, C. H.; Coward, J. K.; Schowen, K. B.; Schowen, R. L. *J. Am. Chem. Soc.* **1979**, *101*, 4351-4358.
(9) Rodgers, J.; Femec, D. A.; Schowen, R. L. *J. Am. Chem. Soc.* **1982**, *104*, 3263-3268.
(10) (a) Pauling, L. "The Nature of the Chemical Bond", 3rd ed.; Cornell University Press: Ithaca, NY, 1960; p 239. (b) Burton, G. W.; Sims, L. B.; Wilson, J. C.; Fry, A. *J. Am. Chem. Soc.* **1977**, *99*, 3371-3379.
(11) Amos, R. D., Cambridge HONDO Mark 1, 1983; a very substantially modified version of King, et al.: King, H. F.; Dupuis, M.; Rys, J. NRCC Software Catalog **1980**, *1*, Program QH02 (HONDO).
(12) Ditchfield, R.; Hehre, W. J.; Pople, J. A. *J. Chem. Phys.* **1971**, *54*, 724-728.
(13) Hehre, W. J.; Stewart, R. F.; Pople, J. A. *J. Chem. Phys.* **1969**, *51*, 2657-2664.
(14) Murtagh, B. A.; Sargent, R. W. H. *Comput. J.* **1970**, *13*, 185.
(15) Schlegel, H. B. *J. Comput. Chem.* **1982**, *3*, 214-218.
(16) Williams, I. H. *J. Mol. Struct. Theochem.* **1983**, *94*, 275-284.
(17) Knowles, P. J., unpublished work.

0002-7863/84/1506-7206$01.50/0

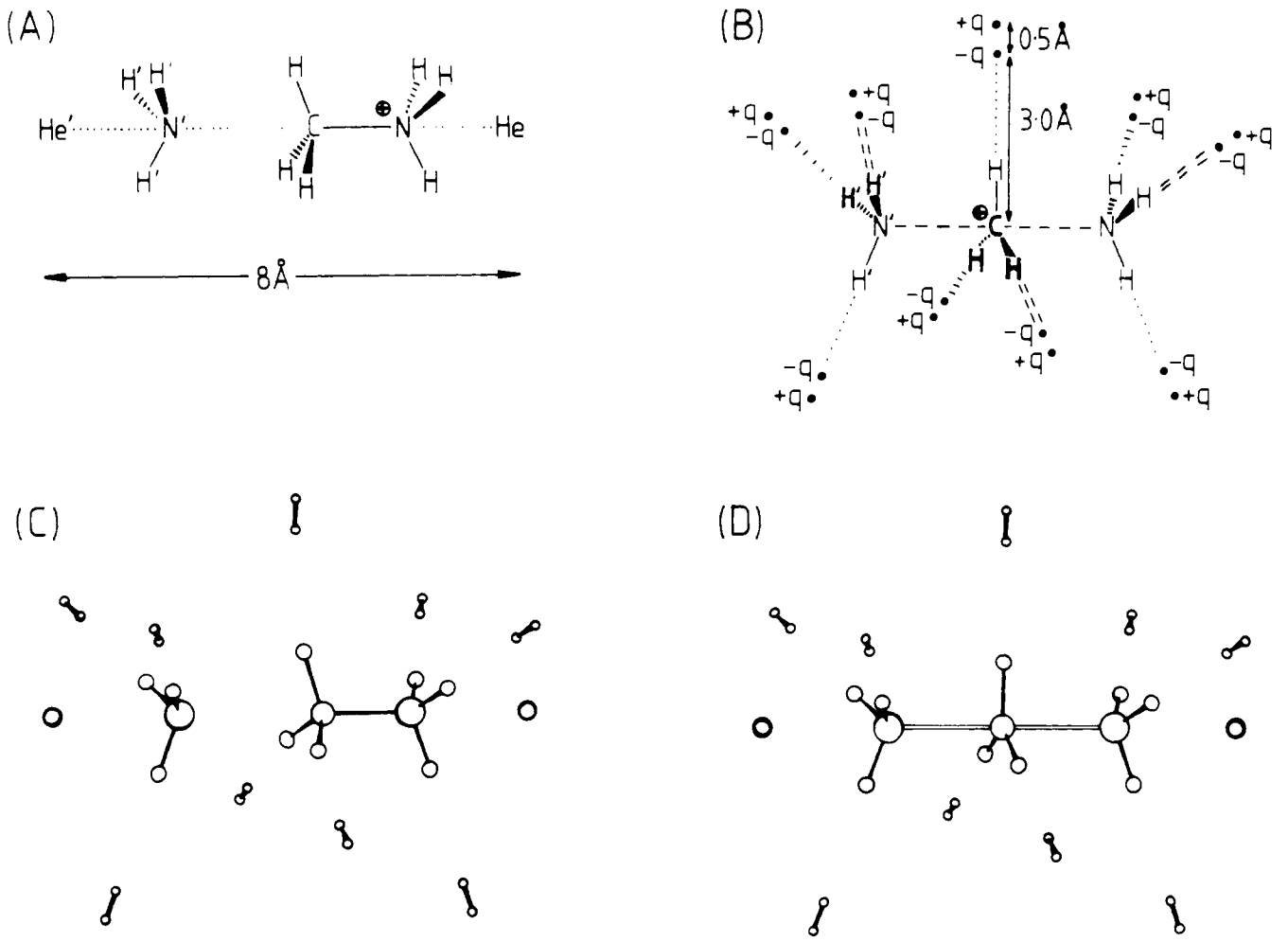

Figure 1. (a) Schematic representation of the reactant complex and the repulsive component of the model catalyst, showing the atomic labeling scheme used in Table I; (b) schematic representation of the transition state and the attractive component of the model catalyst, with q = 0.4e; (c) PLUTO drawing of the reactant complex and the model catalyst; (d) PLUTO drawing of the transition state and the model catalyst.

rotational contributions were projected out from the Cartesian force constants[16] which were then scaled by a factor of 0.82 as described elsewhere.[18] Normal modes and vibrational frequencies were obtained by diagonalization of the matrix of mass-weighted Cartesian force constants.

Molar Gibbs free energies (minus potential energy E) were calculated according to eq 1 where E_{zp} is zero-point energy, q_t, q_r, and q_v are partition functions for translational, rotational, and vibrational motions of ideal-gas molecules, and the superscript symbol degree denotes a standard state of 1 atm. Relative Gibbs free energies in kcal mol^{-1} at 25 °C for standard states of 1 M and 1 mM were then obtained by using eq 2 and 3 where Δn is the stoichiometric change. Kinetic isotope effects were calculated by eq 4.

$$G^\circ - E = E_{zp} + RT \ln (q_t^\circ q_r q_v) \quad (1)$$

$$\Delta G^{1M} = \Delta(G^\circ - E) + \Delta E + 1.89\Delta n \quad (2)$$

$$\Delta G^{1mM} = \Delta G^{1M} - 4.09\Delta n \quad (3)$$

$$k_{light}/k_{heavy} = \exp\{[(-\Delta G^{\circ\ddagger}_{light}) - (-\Delta G^{\circ\ddagger}_{heavy})]/RT\} \quad (4)$$

Model Reaction. The degenerate S_N2 exchange reaction of ammonia (**1**) with methylammonium ion (**2**) (Scheme I) was chosen as the model methyl transfer process for reasons of computational convenience. A threefold symmetry axis along the N··C··N direction is preserved throughout the reaction, and the geometry of the transition structure **4** has D_{3h} symmetry:[19] thus considerable savings were achieved in computations of two-electron integrals and energy gradients during geometry optimization, and also in reducing the number of independent centers to be included in the force-constant calculations, since the HONDO program is able to take advantage of these symmetry elements.

Approach of the neutral nucleophile to the cationic electrophile leads initially to formation of an ion–molecule complex **3** (cf. experimental[20] and theoretical[21] studies on S_N2 reactions of anionic nucleophiles with neutral electrophiles). A central barrier in a symmetric double-well potential separates the narcissistic reactant and product ion–molecule complexes of the uncatalyzed reaction.

Model Catalyst. This comprises two components which contribute (a) a destabilizing interaction and (b) a stabilizing interaction with the reactant, transition structure, and product of the model reaction. (a) The destabilizing component comprises a pair of helium atoms located a fixed distance of 8 Å apart on the N··C··N axis "sandwiching" the reacting system, as shown in Figure 1a. These noble gas atoms serve to provide the mechanical restraint leading to compression by means of purely repulsive (Pauli exclusion principle) interactions with the reacting system. A single STO-2G basis function was used for each helium atom, whose electronic population was found to be 1.974 by Mulliken analysis of the optimized compressed transition-state complex **6**. The repulsive interaction was found to vary approximately as r^{-12}, where r is the He···He separation. The helium atoms are represented schematically as filled circles in Figures 2–4 and Scheme II. (b) The stabilizing component comprises a cage of nine pairs of positive and negative fractional point charges surrounding the reacting system, as shown in Figure 1b. The magnitude of each charge is 0.4 e and the separation within each pair is 0.5 Å, equivalent to a dipole moment of 0.96 D. These dipoles are located along the C–H and N–H bond directions of the compressed

(18) Williams, I. H., manuscript in preparation.

(19) Despite the D_{3h} symmetry of the transition-state geometry, the implicit assumption of transition-state theory that reactants and products are distinguishable requires that an effective rotational symmetry number of 3 (and not 6) is used for evaluation of transition-state partition functions.

(20) Olmstead, W. N.; Brauman, J. I. *J. Am. Chem. Soc.* **1977**, *99*, 4219–4228.

(21) Wolfe, S.; Mitchell, D. J.; Schlegel, H. B. *J. Am. Chem. Soc.* **1981**, *103*, 7692–7694.

Table I. 4-31G Optimized Geometries for Reactant and Transition States of the Model System with and without Compression[a]

		uncompressed		compressed	
coordinate	isolated species **1** and **2**	reactant complex **3**	transition state **4**	reactant complex **5**	transition state **6**
C—N	1.526	1.539	2.092	1.492	1.911
C—N′		3.003	2.092	2.402	1.911
C—H	1.076	1.073	1.062	1.068	1.063
N—H	1.010	1.009	1.003	1 004	1.001
N′—H′	0.991	0.999	1.003	0.998	1.001
N—C—H	108.2	108.4	90.0	107.8	90.0
C—N—H	111.0	110.9	109.3	111.1	109.9
C—N′—H′		107.6	109.3	109.4	109.9
H′—N′—H′	115.8	111.3	109.6	109.6	109.0
He′···N′				2.089	2.089
He′···He				(8.0)[b]	(8.0)[b]

[a] Bond lengths in Å, angles in deg; see Figure 1a for the labeling scheme. [b] Constrained parameter.

transition structure **6**, the distance between the negative point charge and the C or N atom being 3 Å. The cage of point charges is represented schematically as an ellipsoid in **7** and **8** and in Figures 2–4 and Scheme II.

Clearly this model catalyst is not a replica or a realistic likeness of an actual molecular system, nor does it need to be so in order to satisfy its intended purpose. Despite its unusual composition it nonetheless adequately mimics the role which would be played by a more "realistic" molecular model. If it is helpful to imagine a molecular analogy, the model catalyst might be likened to a sort of polycyclic crown ether molecule (cf. dipole moment of diethyl ether = 1.15 D) with repulsive bridgehead interactions.

Catalyst–Substrate Complexes. The geometries of the compressed reactant-state and transition-state structures **5** and **6** (without the cage of point charges) were optimized, in C_{3v} and D_{3h} symmetries, respectively, with the He···He distance constrained at 8 Å. Subsequently Cartesian force constants were computed for each optimized structure, without constraints, and normal-mode analysis performed. Inspection of the resulting normal coordinates and vibrational eigenvalues revealed in each case that the structures were local maxima (on the potential energy surface) with respect to displacements of the reacting system away from the He···He axis. Negative eigenvalues were calculated for two degenerate pairs of linear-bending modes involving the helium atoms, whereas the eigenvalues of the remaining vibrational modes were all positive with one exception: the reaction-coordinate mode of the transition-state complex **6** possessed a negative eigenvalue, as expected.

For the purpose of evaluating vibrational contributions to Gibbs free energy differences (and kinetic isotope effects), the computed negative values of the valence force constants for linear-bending coordinates were replaced by positive values of equal magnitude and all interaction force constants involving these coordinates were set to zero. In order to mimic better the dynamical properties of a small enzyme the helium atoms of the model catalyst were assigned atomic masses of 4000 instead of 4. Of the 42 degrees of freedom of the catalyst–substrate complexes, 30 were internal vibrational motions of the substrate and 6 were translations, rotations, and a vibration of the catalyst. The remaining six degrees of freedom were translational and rotational motions of the substrate within the catalyst–substrate complex, which may be termed as external modes. Force constants were not recomputed for the reactant-state and transition-state complexes **7** and **8** with the complete model catalyst (i.e., for **5** and **6** each within the point-charge cage). Free-energy contributions $G° - E$ for **7** and **8** were assumed to be the same as for **5** and **6**, respectively.

As stated above, the force constants for off-axis translations and rotations of the substrate relative to the catalyst were initially computed to have negative values but were then replaced by equal positive values. This corresponds to the inclusion of a third component of interaction between the model catalyst and the reacting system, viz. a restoring force for off-axis displacements. Such a restoring force is likely to be a feature of any real catalyst and would probably arise largely from steric interactions involving the walls of the binding site. Its implicit inclusion in the present model is therefore entirely reasonable although it does not contribute directly to the catalysis.

Results and Discussion

Optimized geometries and total energies for all species considered in this study are given in Tables I and II. Gibbs free-energy terms $G° - E$ for selected species are given in Table III. Table IV contains kinetic and equilibrium isotope effects calculated for the processes shown in Schemes I and II, and some of these results are further analyzed in Table V.

Table II. Total SCF Energies[a]

	species	sym-metry	energy[b]
1	NH_3	C_{3v}	−56.10669
2	$CH_3NH_3^+$	C_{3v}	−95.44076
	He···He	D_{3h}	−5.40431
3	NH_3···$CH_3NH_3^+$	C_{3v}	−151.56423
4	$[NH_3$--CH_3^+--$NH_3]^‡$	D_{3h}	−151.53444
5	He···NH_3···$CH_3NH_3^+$···He	C_{3v}	−156.92972
6	He···$[NH_3$--CH_3^+--$NH_3]^‡$···He	D_{3h}	−156.90759
	3 + point charges	C_{3v}	−151.62609
	4 + point charges	D_{3h}	−151.58974
7	**5** + point charges	C_{3v}	−156.99353
8	**6** + point charges	D_{3h}	−156.97264
9	distorted **3**	C_{3v}	−151.54944
10	distorted **4**	D_{3h}	−151.52574

[a] 4-31G basis for C, N, and H; STO-2G basis for He. [b] Energies in hartrees.

Table III. Non-Potential-Energetic Contributions to Molar Gibbs Free Energies

	species	$(G° - E)^a$
	He···He	−23.9093
1	NH_3	9.3245
2	CH_3NH_3	34.4584
3	NH_3···$CH_3NH_3^+$	51.8908
4	$[NH_3$--CH_3^+--$NH_3]^‡$	52.4329
5	He···NH_3···$CH_3NH_3^+$···He	44.1295
6	He···$[NH_3$--CH_3^+--$NH_3]^‡$···He	43.9558

[a] Standard state 1 atm, 25 °C; units are kcal mol^{-1}.

Table IV. Calculated Isotope Effects for Methyl Transfer at 25 °C

reaction[a]	type	value[b]	MMI	EXC	ZPE
1 + **2** ⇌ **3**	$K(CH_3)/K(CD_3)$	1.005	1.327	0.788	0.961
3 → **4**‡	$k(CH_3)/k(CD_3)$	0.913	0.991	1.093	0.843
1 + **2** → **4**‡	$k(CH_3)/k(CD_3)$	0.918	1.315	0.861	0.810
	$k(^{12}C)/k(^{13}C)$	1.064	1.042	0.981	1.040
	$k(^{12}C)/k(^{14}C)$	1.123	1.082	0.963	1.078
3 ⇌ **5**	$K(CH_3)/K(CD_3)$	0.812	1.101	0.979	0.754
5 → **6**‡	$k(CH_3)/k(CD)_3$	0.872	0.993	1.079	0.814
	$k(^{12}C)/k(^{13}C)$	1.072	1.000	1.010	1.061
	$k(^{12}C)/k(^{14}C)$	1.140	1.000	1.020	1.117

[a] See Scheme I. [b] Isotope effect = (MMI)(EXC)(ZPE).

Table V. Analysis of ZPE Factors Contributing to Calculated α-D_3 Isotope Effects

modes	uncatalyzed KIE **3** → **4**‡	catalyzed KIE **5** → **6**‡	modes	substrate binding EIE **3** ⇌ **5**
CH str.	0.786	0.926	CH str.	0.925
CH def.	1.339	1.360	CH bends	0.924
CH rock	2.585	2.038	others:	
NH rock	0.296	0.300	internal	0.917
others	1.047	1.061	external	0.962
all	0.843	0.814	all	0.754

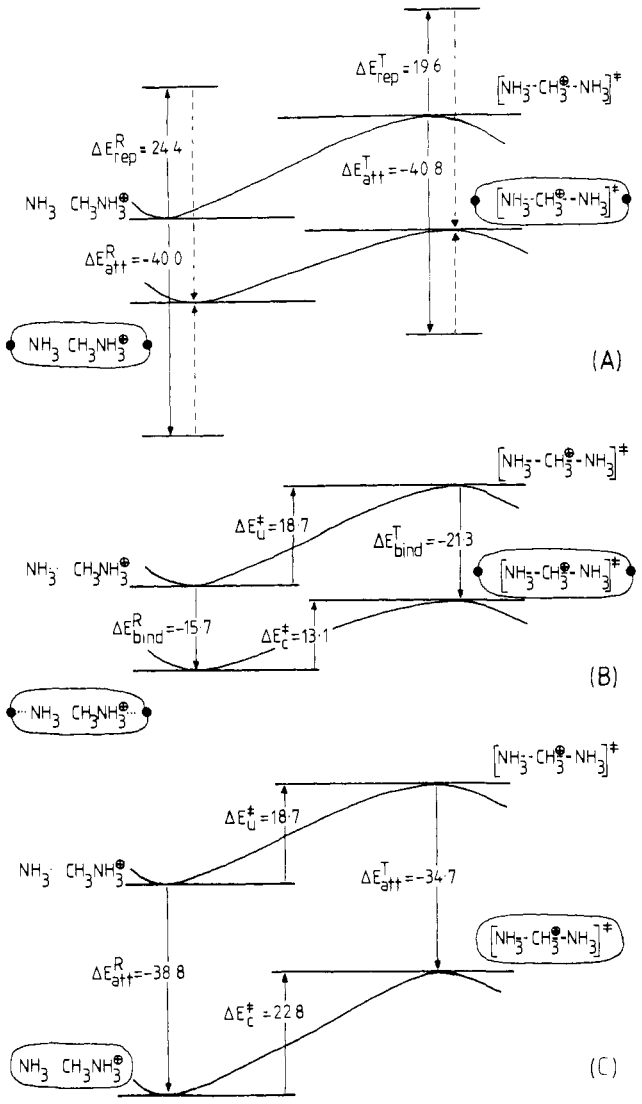

Figure 2. (a) Repulsive and attractive component interaction potential energies for the catalyzed model reaction; (b) total interaction potential energies for the model reaction catalyzed with compression; (c) potential energies of interaction for the model reaction "catalyzed" in the absence of compression.

Geometrical Consequences of Compression. Progress from the reactant complex **3** to the transition structure **4** of the uncatalyzed methyl transfer is accompanied by a decrease in the sum of the making and breaking C–N bond lengths (i.e., the distance N′···N) from 4.54 to 4.18 Å. Pauling bond orders[10] B_{CN} may be calculated by eq 5 where R_B is the length of a C–N bond of order B and R_1 is the length of a C–N bond of unit order. Thus the bond orders for the making and breaking C–N bonds of the uncompressed

$$B_{CN} = \exp[(R_1 - R_B)/0.3] \qquad (5)$$

system are respectively 0.01 and 0.79 in the reactant complex and 0.13 each in the transition structure, characterizing a very loose transition state. The optimized bond lengths and angles given in Table I for the reaction catalyzed with compression show that the making C–N′ and breaking C–N bonds of the reactant complex **5** are shortened by 0.60 and 0.05 Å, respectively, from their uncompressed values, corresponding to increased bond orders of 0.04 and 0.93. Progress from the reactant complex **5** to the transition structure **6** is accompanied by reduction of the N′···N distance from 3.89 to 3.82 Å, a much smaller decrease than for the uncompressed reaction. The transition-state bond orders B_{CN} = 0.23 for **6** indicate a tighter structure than for **4**. These calculated C–N bond orders of 0.23 and 0.13 respectively for the compressed and uncompressed transition states are much lower than the previously inferred[9] equal bond orders B_{CO} and B_{CS} of

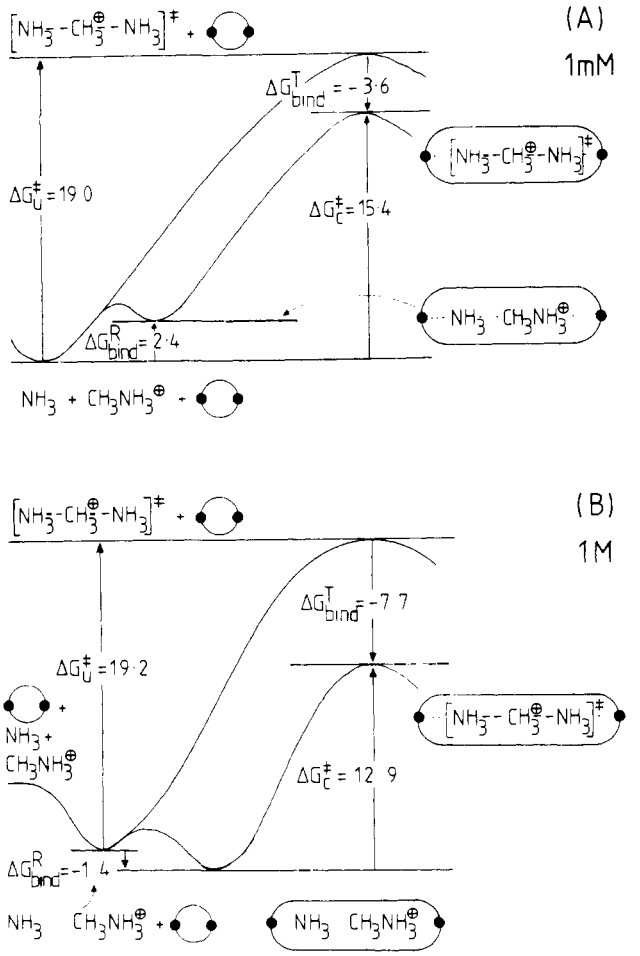

Figure 3. Gibbs free energy changes at 25 °C for the model reaction catalyzed with compression at standard states of (a) 1 mM and (b) 1 M.

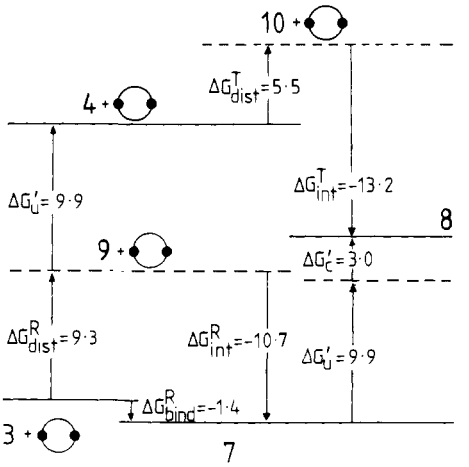

Figure 4. Gibbs free energy changes at 25 °C and 1 M illustrating the canonical view of catalysis with compression. (See Scheme I for identification of structures.)

0.55 and 0.45 for the enzymic and non-enzymic transition states for methyl transfer between sulfur and oxygen atoms. This discrepancy is probably a reflection of the fact that the calculated model methyl transfer occurs in vacuo whereas the experimental data are from reactions in condensed media. Nonetheless, it may be noted that in both cases the effect of compression is to increase the transition-state bond orders by 0.1.

Viewed in another way, the effect of compression is to reduce the reactant-state N′···N distance by 0.65 Å but the transition-state N′···N distance by only 0.36 Å. It will be seen below that this greater distortion in the reactant complex than in the transition state incurs a correspondingly greater energetic penalty.

Potential Energies. The reactant ion–molecule complex **3** for the uncatalyzed process is stabilized with respect to **1** and **2** by 10.5 kcal mol^{-1}, and a potential energy barrier of 18.7 kcal mol^{-1} separates this species from the mirror-image product complex. These numbers are not given as accurate estimates of the ion–molecule association energy and intrinsic energy barrier for the gas-phase reaction. It is likely that use of a larger basis set would increase the intrinsic barrier whereas inclusion of electron correlation would decrease it, as found for proton transfer.[22] Interestingly though, Scheiner et al.[22] found that the 4-31G level of SCF theory yields intrinsic barriers to proton transfer in agreement with the results of a much more sophisticated treatment using third-order Møller–Plesset theory with a polarized triple-valence 6-311G** basis. Thus, although the energies presented here are only intended to be of qualitative significance within the model for catalysis, they are nonetheless probably quite plausible.

The interaction energy of the reactant (or product) complex with the model catalyst may be expressed as the sum of repulsive and attractive components. The repulsive interaction with the pair of helium atoms destabilizes the reactant complex by 24.4 kcal mol^{-1} whereas the attractive interaction with the cage of point charges stabilizes the compressed reactant complex by 40.0 kcal mol^{-1}. The total reactant-state binding energy is thus given by eq 6. Similarly the transition state is destabilized by the helium

$$\Delta E^{R}_{bind} = \Delta E^{R}_{rep} + \Delta E^{R}_{att} = 24.4 + (-40.0) = -15.7 \text{ kcal mol}^{-1} \quad (6)$$

atoms by 19.6 kcal mol^{-1}, but the point charges stabilize it by 40.8 kcal mol^{-1}, so that the total transition-state binding energy is given by eq 7. The component and total interaction energies are shown in Figure 2, parts a and b.

$$\Delta E^{T}_{bind} = \Delta E^{T}_{rep} + \Delta E^{T}_{att} = 19.6 (-40.8) = -21.3 \text{ kcal mol}^{-1} \quad (7)$$

The potential energy barrier $\Delta E^{\ddagger}_{c}$ for the reaction catalyzed with compression may be found as eq 8, where $\Delta E^{\ddagger}_{u}$ is the barrier height for the uncatalyzed model reaction. Rearrangement of

$$\Delta E^{\ddagger}_{c} = \Delta E^{\ddagger}_{u} - \Delta E^{R}_{bind} + \Delta E^{T}_{bind} \quad (8)$$

$$\Delta E_{cat.} = \Delta E^{\ddagger}_{u} - \Delta E^{\ddagger}_{c} = \Delta E^{R}_{bind} - \Delta E^{T}_{bind} = -15.7 - (-21.3) = 5.6 \text{ kcal mol}^{-1} \quad (9)$$

eq 8 allows the potential energetic contribution to catalysis $\Delta E_{cat.}$ to be determined. This positive quantity indicates a catalytic effect due to a reduced potential energy barrier height.

It is of interest to ask what sort of catalysis there might be in the absence of compression, by considering only the attractive interaction energies of the uncompressed reactant complex and transition structure with the cage of point charges. These interactions are shown in Figure 2c. Now the barrier height for the "catalyzed" reaction is given by eq 10 and the magnitude of

$$\Delta E^{\ddagger}_{c} = \Delta E^{\ddagger}_{u} - \Delta E^{R}_{att} + \Delta E^{T}_{att} \quad (10)$$

$$\Delta E_{cat.} = \Delta E^{R}_{att} - \Delta E^{T}_{att} = -38.8 - (-34.7) = -4.1 \text{ kcal mol}^{-1} \quad (11)$$

the "catalysis" by eq 11. The negative sign of $\Delta E_{cat.}$ implies *anticatalysis*, or inhibition, since the potential energy barrier height has been increased by interaction with the point charges. The model catalyst only operates as a catalyst provided that the destabilizing interactions with the helium atoms are expressed. In other words, for this model methyl transfer there is *no catalysis without compression*. The origin of the catalysis is the less unfavorable interaction of the helium atoms with the reacting system in the transition state than in the reactant state: it costs more to distort the latter than the former.

(22) Scheiner, S.; Szczesniak, M. M.; Bigham, L. D. *Int. J. Quantum Chem.* **1983**, *23*, 739–751.

Scheme II

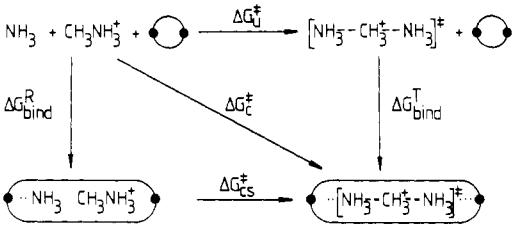

Since $\Delta E^{R}_{att} \simeq \Delta E^{T}_{att}$, the difference $\Delta E^{R}_{rep} - \Delta E^{T}_{rep}$ is a good approximation to the catalytic potential energy $\Delta E_{cat.}$. As the distance r between the helium atoms is changed so therefore the magnitude of $\Delta E_{cat.}$ varies roughly as r^{-12}. Decreasing r by 0.1 Å would lead to an increase in $\Delta E^{R}_{rep} - \Delta E^{T}_{rep}$ of about 0.8 kcal mol^{-1}, contributing a further factor of about 4 to the rate enhancement at 25 °C; decreasing r to 7.55 Å would double $\Delta E^{R}_{rep} - \Delta E^{T}_{rep}$ resulting in roughly a 3300-fold extra rate enhancement.

Gibbs Free Energies. Molar Gibbs free energies $G° - E$ (minus potential energy) for each component of the model methyl transfer at 25 °C are given in Table III. Scheme II shows the free energies of activation and of binding pertinent to a discussion of the catalysis of the reaction. The activation energy $\Delta G^{\ddagger}_{cs}$ for the catalyst–substrate complex is independent of the choice of standard state since $\Delta n = 0$ in eq 2 and 3, but the other terms are standard-state dependent with $\Delta n = -1$.

Figure 3a illustrates the free energy changes at 25 °C with each component at a concentration of 1 mM. Under these conditions the binding energy ΔG^{R}_{bind} of the free reactants with the catalyst is 2.4 kcal mol^{-1}, implying a dissociation constant $K_m = 62$ mM^2 so that there is no substantial concentration of catalyst–substrate complex. The activation free energy of 15.4 kcal mol^{-1} for the catalyzed reaction is thus the sum of $\Delta G^{\ddagger}_{cs}$ with ΔG^{R}_{bind}, eq 12, and is equal to the sum of the transition-state binding energy with the activation energy for the uncatalyzed reaction. The catalytic

$$\Delta G^{\ddagger}_{c} = \Delta G^{R}_{bind} + \Delta G^{\ddagger}_{cs} = \Delta G^{\ddagger}_{u} + \Delta G^{T}_{bind} \quad (12)$$

free energy, $\Delta G_{cat.}$, is the difference between the activation free energies of the catalyzed and uncatalyzed reactions. According to eq 13, *all* of the transition-state binding energy is expressed as catalytic free energy.

$$\Delta G_{cat.} = \Delta G^{\ddagger}_{u} - \Delta G^{\ddagger}_{c} = -\Delta G^{T}_{bind} = 3.6 \text{ kcal mol}^{-1} \quad (13)$$

The free energy changes for a standard state of 1 M are shown in Figure 3b. The reactant state for the uncatalyzed process is effectively the ion–molecule complex since this is stabilized by 4.3 kcal mol^{-1} with respect to ammonia and methylammonium. The dissociation constant K_m for the catalyst–substrate complex is 0.09 M so now the catalyst–substrate complex is the predominant reactant-state species for the catalyzed methyl transfer and the relevant activation free energy is $\Delta G^{\ddagger}_{cs}$. The catalytic free energy is therefore given by eq 14, and it is equivalent to a rate acceleration of 4.2×10^4 at 25 °C. As is clear from Figure 3b,

$$\Delta G_{cat.} = \Delta G^{\ddagger}_{u} - \Delta G^{\ddagger}_{cs} = 19.2 - 12.9 = 6.3 \text{ kcal mol}^{-1} \quad (14)$$

$$\Delta G_{cat.} = \Delta G^{R}_{bind} - \Delta G^{T}_{bind} = -1.4 + 7.7 \text{ kcal mol}^{-1} \quad (15)$$

$\Delta G_{cat.}$ is also equal to the negative difference between the binding energies of the transition state and of the reactant state, eq 15. It may be seen that, at saturating substrate concentrations, the reactant-state binding energy is actually *inhibitory* in character. This term subtracts from the transition-state binding energy to yield a smaller catalytic free energy. Clearly catalysis is most effective when ΔG^{R}_{bind} is a minimum so that the full contribution of ΔG^{T}_{bind} may be expressed.

Fundamentalist and Canonical Descriptions of Catalysis with Compression. A "Fundamentalist" approach to catalysis has been adopted implicitly in the foregoing discussion, i.e. the position "that

the entire and sole source of catalytic power is the stabilization of the transition state; that reactant-state interactions are by nature inhibitory and only waste catalytic power".[23] Thus the importance of ΔG^{T}_{bind} in determining the catalytic free energy has been demonstrated. A "canonical" view[23] of catalysis with compression would be to regard it as an example of a reactant-state destabilization mechanism (cf. ref 24). It may be imagined that the reaction follows a path along which the reactants adopt a particular unstable structure **9** having the same geometry as the reactant-derived portion of the catalyst–substrate complex **7**. The free energy required to distort the reactants in this manner is ΔG^{R}_{dist}. It may then be imagined that the distorted structure **9** binds with the catalyst to form **7**; the interaction energy ΔG^{R}_{int} is the intrinsic binding energy of **9**. The sum of ΔG^{R}_{dist} and ΔG^{R}_{int} is the net reactant-state binding energy ΔG^{R}_{bind} mentioned in the previous section. If it is assumed that the non-potential-energetic term ($G^\circ - E$) is the same for the formal transformation **3** → **9** as for **3** → **4**, then a free energy diagram (Figure 4) may be constructed to illustrate the canonical description of catalysis under saturating conditions.

If the role of the catalyst were merely to bind the reactants in their distorted (destabilized) form **9**, then the intrinsic binding energy would retain the same value at all points along the reaction coordinate and, in particular, ΔG^{R}_{int} would equal ΔG^{T}_{int} at the transition state. Moreover, the activation free energy for the catalyzed reaction would then be the same as the free energy change $\Delta G'_u$ required to take the distorted reactants **9** to the transition state **4** for the uncatalyzed reaction. In this case the catalytic free energy would be equal to the distortion energy (eq 16): $\Delta G_{cat.}$ would be the negative of that part of ΔG^{R}_{int} (the "utilized" part) which "pays off" the energetic cost of ΔG^{R}_{dist}.

$$\begin{aligned}\Delta G_{cat.} &= \Delta G^{\ddagger}_{u} - \Delta G^{\ddagger}_{c} \\ &= \Delta G^{R}_{dist} + \Delta G'_{u} - \Delta G'_{u}\end{aligned} \quad (16)$$

In the present example, however, the geometry of the transition state **4** for the uncatalyzed reaction is not the same as that of the substrate-derived portion (**10**) of the transition state **8** for the catalyzed reaction. The distortion energy required to effect the formal transformation **4** → **10** is ΔG^{T}_{dist}. Furthermore, the intrinsic binding energy ΔG^{T}_{int} of the distorted transition-state structure **10** with the catalyst is not the same as ΔG^{R}_{int}. As Figure 4 shows, the activation free energy for the catalyzed reaction is equal to $\Delta G'_u$ plus a further contribution $\Delta G'_c$ given by eq 17.

$$\begin{aligned}\Delta G'_c &= \Delta G^{T}_{dist} + \Delta G^{T}_{int} - \Delta G^{R}_{int} \\ &= 5.5 + (-13.2) - (-10.7) = 3.0 \text{ kcal mol}^{-1}\end{aligned} \quad (17)$$

Hence the catalytic free energy is given by eq 18 which may be seen to reduce to the Fundamentalist eq 13. The Fundamentalist

$$\begin{aligned}\Delta G_{cat.} &= (\Delta G^{R}_{dist} + \Delta G'_{u}) - (\Delta G'_{u} - \Delta G'_{c}) \\ &= (\Delta G^{R}_{dist} + \Delta G^{R}_{int}) - (\Delta G^{T}_{dist} + \Delta G^{T}_{int}) \\ &= \Delta G^{R}_{bind} - \Delta G^{T}_{bind}\end{aligned} \quad (18)$$

and canonical descriptions are equivalent in that they both lead to the same result in the end. However, the latter description is complicated, relative to the former, by the involvement not only of the distorted reactant structure **9** but also of the distorted transition structure **10**. Since eq 18 shows that it is incorrect to ascribe the source of catalytic power merely to reactant-state destabilization, i.e., $\Delta G_{cat.} \neq \Delta G^{R}_{dist}$, it would seem to be unhelpful to employ the canonical description which tends to emphasize the interaction of the catalyst with the reactants rather than with the transition state.

There is an analogy between, on the one hand, the canonical concept of the unliberated part of the intrinsic binding energy paying off the energy needed to destabilize the reactants in the catalyzed process and, on the other hand, the opposition of attractive and repulsive catalyst–substrate interactions built into the present model for catalysis with compression. Unfortunately the apparent fit between canonical terminology and the roles of the dual components of the model catalyst does not bear up to closer scrutiny. Superficially it might appear that the agent for destabilization would be the repulsive interaction with the catalyst; however, ΔE^{R}_{dist} = 9.3 kcal mol^{-1} whereas ΔE^{R}_{rep} = 24.4 kcal mol^{-1}, and ΔE^{T}_{dist} = 5.5 kcal mol^{-1} but ΔE^{T}_{rep} = 19.6 kcal mol^{-1}. Similarly the intrinsic binding energies may not be imagined as arising simply from the attractive interactions since ΔE^{R}_{int} = −25.0 kcal mol^{-1} and ΔE^{T}_{int} = −26.7 kcal mol^{-1} but ΔE^{R}_{att} = −40.0 kcal mol^{-1} and ΔE^{T}_{att} = −40.8 kcal mol^{-1}. An accurate description of catalysis by compression should consider energetic differences between reactants and transition states; in this respect it may be noted that the differential repulsive interaction $\Delta E^{R}_{rep} - \Delta E^{T}_{rep}$ = 4.8 kcal mol^{-1} is quite similar to the difference of 3.8 kcal mol^{-1} between ΔE^{R}_{dist} and ΔE^{T}_{dist}.

Kinetic Isotope Effects. The molar Gibbs free energies reported in Table III for standard isotopic species were recomputed for isotopomers in which the transferring methyl group was in turn labeled with three deuterium atoms and with carbon-13 and carbon-14. Kinetic isotope effects $k(CH_3)/k(CD_3)$, $k(^{12}C)/k(^{13}C)$, and $k(^{12}C)/k(^{14}C)$ at 25 °C were calculated according to eq 4 and are given in Table IV. The kinetic isotope effects (KIE) calculated for the uncatalyzed model reaction are entirely consistent with experimental results for other S_N2 methyl transfers (cf. ref 25). For example, reaction of methyl iodide with pyridine in benzene gives $k(CH_3)/k(CD_3)$ = 0.919 ± 0.002 at 50 °C[26] and $k(^{12}C)/k(^{14}C)$ = 1.142 + 0.009 at 25 °C[27] as compared with calculated values of 0.918 and 1.123, respectively, for the uncatalyzed model reaction **1** + **2** → **4**‡ at 25 °C. The overall inverse α-D_3 KIE for **1** + **2** → **4**‡ is the product of an equilibrium isotope effect (EIE) of 1.005 for the association **1** + **2** ⇌ **3** and a slightly more inverse KIE of 0.913 for **3** → **4**‡. The small normal value of this EIE for association arises from a large normal mass-and-moment-of-inertia (MMI) factor which is not quite balanced by inverse excitational (EXC) and zero-point energy (ZPE) factors. As expected, the inverse KIE for **3** → **4**‡ is due to an appreciably inverse ZPE term, somewhat offset by a normal EXC factor. This ZPE term may be further analyzed into contributions from particular groups of normal modes, as in Table V. The degenerate rocking modes of the CH_3 and the leaving NH_3 groups are highly coupled and their frequencies are both very isotopically sensitive. The normal ZPE factor from the CH bending modes is almost exactly cancelled by an inverse factor from the NH rocking modes, and the overall product is determined mainly by the (surprisingly) inverse contribution from the CH stretching modes.

Schowen and co-workers[7] determined $V_{max}^{CH_3}/V_{max}^{CD_3}$ = 0.86 ± 0.03 for methylation of 3,4-dihydroxyacetophenone with *S*-adenosylmethionine at 37 °C and pH 7.58 catalyzed by rat-liver catechol *O*-methyl transferase (COMT). This is an isotope effect upon $\Delta G^{\ddagger}_{ES}$, the free energy of activation of the enzyme–substrate complex, which corresponds to the isotope effect upon $\Delta G^{\ddagger}_{CS}$ (see Scheme II) for the model catalyzed reaction, i.e., the KIE for **5** → **6**‡, which is calculated to be 0.872 at 25 °C. The absolute values of these KIEs for COMT-catalyzed and model-catalyzed methyl transfers may not be compared directly since both the catalysts and the catalyzed reactions are obviously quite different. However, it is significant that both KIEs are appreciably more inverse than for their respective uncatalyzed model reactions: $k(CH_3)/k(CD_3)$ = 0.97 ± 0.02 for methylation of methoxide ion by *S*-methyldibenzothiophenium ion at 25 °C in methanol[8] and $k(CH_3)/k(CD_3)$ = 0.918 for **1** + **2** → **4**‡. It may be presumed that the more inverse KIEs for both catalyzed processes arise as the result of a *functional* similarity between COMT and the model catalyst, i.e., as a consequence of catalysis with compression both

(23) Schowen, R. L. In "Transition States of Biochemical Processes"; Gandour, R. D., Schowen, R. L., Eds.; Plenum Press: New York, 1978.

(24) Jencks, W. P. *Adv. Enzymol. Relat. Areas Mol. Biol.* **1975**, *43*, 219–410.

(25) Melander, L.; Saunders, W. H. "Reaction Rates of Isotopic Molecules"; Wiley-Interscience: New York, 1980.

(26) Leffek, K. T.; McLean, J. W. *Can. J. Chem.* **1965**, *43*, 40–46.

(27) Bender, M. L.; Hoeg, D. F. *J. Am. Chem. Soc.* **1957**, *79*, 5649–5654.

by the enzyme and by the model catalyst.

The calculated KIE for $5 \rightarrow 6^{\ddagger}$ is dominated by the ZPE factor which is further analyzed in Table V. The major change in the ZPE factors for $5 \rightarrow 6^{\ddagger}$ vs. $3 \rightarrow 4^{\ddagger}$ is the smaller normal contribution from the CH rocking modes. The frequencies for these modes decrease as between reactants and transition state for both the catalyzed and uncatalyzed model reactions, but the size of the decrease is smaller in the case of catalysis with compression. Thus the overall ZPE factor for $5 \rightarrow 6^{\ddagger}$ is more inverse than that for $3 \rightarrow 4^{\ddagger}$.

The isotope effect $(V_{max}/K_m)^{CH_3}/(V_{max}/K_m)^{CD_3}$ determined by Schowen and co-workers[7] for the COMT-catalyzed reaction did not differ sensibly from the isotope effect $V_{max}^{CH_3}/V_{max}^{CD_3}$, implying that there was no α-D_3 isotope effect for binding of *S*-adenosylmethionine to the enzyme. As Table IV shows, however, there is a substantial calculated α-D_3 EIE of 0.812 for the equilibrium $3 \rightleftharpoons 5$ for binding of the reactant complex to the model catalyst. The error bounds for one standard deviation on the experimental $(V_{max}/K_m)^{CH_3}/(V_{max}/K_m)^{CD_3}$ value are actually sufficiently large as to permit the possibility of an inverse EIE for cofactor binding as large as the value calculated here for the model system; but since the nature of the binding interactions is certainly very different in the enzyme and in the model catalyst, it is perhaps not very remarkable if the EIEs for substrate binding are indeed significantly different.

Table IV also contains carbon-13 and carbon-14 KIEs calculated for the model methyl transfers. The value of $k(^{12}C)/k(^{13}C) = 1.072$ for the catalyzed process $5 \rightarrow 6^{\ddagger}$ is slightly larger than the value of 1.064 for the uncatalyzed reaction $1 + 2 \rightarrow 4^{\ddagger}$. The ZPE factor is dominating for both isotope effects. The experimental carbon-13 isotope effects are $V_{max}^{12}/V_{max}^{13} = 1.14 \pm 0.14$ for the COMT-catalyzed reaction[7] and $k(^{12}C)/k(^{13}C) = 1.08 \pm 0.02$ for methylation of methoxide by *S*-methyldibenzothiophenium tetrafluoroborate.[8] Thus the KIE for the enzyme-catalyzed reaction is probably larger than that for the uncatalyzed reaction, in accord with the results of the calculations for the model system. Once again it may be supposed that this similarity derives from the operation of a catalytic mechanism involving compression both for the COMT enzyme and for the model catalyst.

Conclusions

Despite its simplicity the model catalyst described in this work has successfully demonstrated the viability of catalysis of methyl transfer by a compression mechanism. It has been shown that the greater energetic penalty incurred by a compressed reactant state than by a compressed transition state allows the latter to be stabilized preferentially by a suitably designed catalyst, thereby causing a reduction in the activation energy. Preferential transition-state binding by the model catalyst does not occur in the absence of compression by repulsive interactions; on the contrary, the model reaction is actually inhibited by a "catalyst" which binds its substrates by attractive interactions only. Kinetic isotope effects calculated for catalyzed and uncatalyzed model reactions are in accord with trends in experimental isotope effects for enzymic and non-enzymic methyl transfers. Thus the theoretical model lends support to Schowen's hypothesis[5] concerning the possible role of compression in enzymic catalysis of methyl transfer. The importance of repulsive interactions between the catalyst and the substrate, at least for this class of group-transfer process, may have more general implications for design of synthetic catalysts. Simple juxtaposition of a catalytic site with a binding site affording attractive interactions only with a substrate may not necessarily permit differential binding (in the desired sense!) as between the reactant state and the transition state so as to provide catalysis.

Conformations of Cyclic Octapeptides. 1

Kenneth D. Kopple,* Kumarapuram N. Parameswaran, and James P. Yonan

Contribution from the Department of Chemistry, Illinois Institute of Technology, Chicago, Illinois 60616. *Received February 29, 1984*

Abstract: Four diastereoisomeric cylic octapeptides, *cyclo*(L- or D-Ala-Gly-L-Pro-L- or D-Phe)$_2$, were synthesized and characterized, and NMR data bearing on their conformations in dimethyl sulfoxide solution were obtained. The most stable backbones of these peptides have trans Gly–Pro peptide bonds and C_2 symmetry in the NMR average. The populations of the all-trans C_2 form range between 50 and 98%. Likely solution conformations of all-trans *cyclo*(D-Ala-Gly-L-Pro-D-Phe)$_2$ and *cyclo*(L-Ala-Gly-L-Pro-L-Phe)$_2$ have turns at Pro-Phe. In both peptides two planes containing sequences of Gly, Pro, Phe, and Ala α-carbons are joined at roughly right angles along a line between the Ala α-carbons, and the Ala methyl groups are directed toward each other across the ring on the convex side of the fold. The proposed conformation for *cyclo*(L-Ala-Gly-L-Pro-L-Phe)$_2$ has two type I L-Pro-L-Phe β turns and is similar in important respects to the backbone of the crystalline cyclic octapeptide β-amanitin, except that β-amanitin contains both type I and type II turns. Data are presented for *cyclo*(L-Ala-Gly-L-Pro-D-Phe)$_2$, but a closely defined conformation is not obvious from them. Conformations of *cyclo*(D-Ala-Gly-L-Pro-L-Phe)$_2$ will be described in a subsequent paper.

Synthetic cyclic peptides of defined backbone conformation are potentially useful as analogues for determining biologically active conformations of naturally occurring peptides. Considerable progress has been made through NMR and X-ray investigations in determining the rules governing the relation between sequence and stable conformation for cyclic penta- and hexapeptides, particularly those containing the β turn as a well-defined conformational feature.[1-5] Because other cyclic peptide backbones may be of service as well, we now report studies to identify sequences producing stable cyclic octapeptide backbone conformations.

We desired to produce cyclic octapeptide backbones of C_2 symmetry determined by two β turns, using proline residues to locate the turns. Because the conformation of a peptide chain is determined to a first approximation by the sequence of glycines, prolines, and residues with a β-carbon, and by the α-carbon

(1) Gierasch, L. M.; Deber, C. M.; Madison, V.; Niu, C.-H.; Blout, E. R. *Biochemistry* **1981**, *20*, 4730-4738.
(2) Kopple, K. D. *Biopolymers* **1981**, *20*, 1913-1920.
(3) Bara, Y.; Friedrich, A.; Hehlein, W.; Kessler, H.; Kondor, P.; Molter, M.; Veith, H.-J. *Chem. Ber.* **1978**, *111*, 1045-1057.
(4) Pease, L. G.; Niu, C.-H.; Zimmermann, G. *J. Am. Chem. Soc.* **1979**, *101*, 184-191.
(5) Ovchinnikov, Yu. A.; Ivanov, V. T. "The Proteins", 3rd ed.; "The Cyclic Peptides: Structure, Conformation and Function", Neurath, H., Hill, R. L., Eds.; Academic Press: New York, 1980; Vol. 5, pp 491-538.

0002-7863/84/1506-7212$01.50/0